Mimivirus encodes a multifunctional primase with DNA/RNA polymerase, terminal transferase and translesion synthesis activities

Ankita Gupta[1,†], Shailesh B. Lad[1,†], Pratibha P. Ghodke[2], P.I. Pradeepkumar[2] and Kiran Kondabagil [1,*]

[1]Department of Biosciences and Bioengineering, Indian Institute of Technology Bombay, Powai, Mumbai, Maharashtra 400076, India and [2]Department of Chemistry, Indian Institute of Technology Bombay, Powai, Mumbai, Maharashtra 400076, India

ABSTRACT

Acanthamoeba polyphaga **mimivirus is an amoeba-infecting giant virus with over 1000 genes including several involved in DNA replication and repair. Here, we report the biochemical characterization of gene product 577 (gp577), a hypothetical protein (product of L537 gene) encoded by mimivirus. Sequence analysis and phylogeny suggested gp577 to be a primase-polymerase (PrimPol)—the first PrimPol to be identified in a nucleocytoplasmic large DNA virus (NCLDV). Recombinant gp577 protein purified as a homodimer and exhibited** *de novo* **RNA as well as DNA synthesis on circular and linear single-stranded DNA templates. Further, gp577 extends a DNA/RNA primer annealed to a DNA or RNA template using deoxyribonucleoties (dNTPs) or ribonucleotides (NTPs) demonstrating its DNA/RNA polymerase and reverse transcriptase activity. We also show that gp577 possesses terminal transferase activity and is capable of extending ssDNA and dsDNA with NTPs and dNTPs. Mutation of the conserved primase motif residues of gp577 resulted in the loss of primase, polymerase, reverse transcriptase and terminal transferase activities. Additionally, we show that gp577 possesses translesion synthesis (TLS) activity. Mimiviral gp577 represents the first protein from an NCLDV endowed with primase, polymerase, reverse transcriptase, terminal transferase and TLS activities.**

INTRODUCTION

Accurate genome duplication requires DNA replication machinery to copy the genome with high fidelity and includes DNA damage repair before the intact genome is passed on to the daughter cells [1]. The primary enzymes involved in the replication process include helicase, topoisomerase, primase, ligase and DNA-dependent DNA polymerases. A primase is a DNA-dependent RNA polymerase essential for replication initiation [2]. DNA polymerases are incapable of *de novo* DNA synthesis and hence, utilize the free 3′ hydroxyl group produced by the primase [2]. Primases are broadly categorized as bacterial primases belonging to the dnaG superfamily or the archaeo-eukaryotic primase (AEP) superfamily [3,4]. Although performing similar functions, these two families of proteins are structurally different. The dnaG family proteins consist of a conserved topoisomerase-primase fold that forms the TOPRIM domain, whereas AEPs contain an RNA recognition motif (RRM) that forms the catalytic core. AEPs are distributed widely across all domains of life and a few well-characterized examples include human coiled-coil domain containing (CCDC111) protein [5], PrimPol-like protein PPL1 of *Trypanosoma brucei* [6], archaeal PrimPols such as ORF904 encoded by pRN1 plasmid of crenarchaeote *Sulfolobus islandicus* [7], PriS of *Pyrococcus furiosus* [8] and PriS/L complexes of *Pyrococcus horikoshii* [9], *Sulfolobus solfataricus* [10], *Thermococcus kodakaraensis* [11] and *Archaeoglobus fulgidus* [12]. Viral genomes also encode AEP-like proteins, for instance, the herpes simplex virus type I (HSV-I), a large dsDNA virus, contains a UL5-UL8-UL52 heterotrimeric primase-helicase complex where UL52 serves as the AEP essential for priming DNA replication [13]. Additionally, the D5-protein of vaccinia virus [14,15], a large DNA virus and Lef-1 protein of baculoviruses are examples of viral AEPs [16].

PrimPols are members of the AEP superfamily that catalyzes the synthesis of short RNA and/or DNA primers and also possess DNA-dependent DNA polymerase activi-

ties ([5–7](#),[17–19](#)). The replication protein ORF904 of pRN1 plasmid was the first PrimPol to be functionally characterized ([7](#)). Interestingly, archaeal primases such as PriS/L encoded by *Sulfolobus solfataricus* genome ([10](#)), Rep245 and PolpTN2 encoded by the plasmids of *Sulfolobus solfataricus* ([20](#)) and *Thermococcus nautilus* ([21](#)), respectively possess the 3′-terminal deoxynucleotidyl transferase (TdT) activity. The sole reported example of a PrimPol-like enzyme from a virus is the gp43 protein of corynephage BFK20 ([22](#)). The primase and polymerase activities reside in the N-terminal PrimPol-like domain of this protein, whereas the C-terminal possesses a helicase domain ([22](#)). Such PrimPol like proteins with versatile nucleotidyl transferase activities could be major players in DNA replication and related processes.

Viruses are known to use the host replication, transcriptional and translational machinery for the propagation of their progeny but *Acanthamoeba polyphaga* mimivirus, a nucleocytoplasmic large DNA virus (NCLDV) with 1.2 Mb genome ([23](#)) encodes several proteins involved in these processes ([24](#)). Iyer *et al.*, on the basis of sequence features, had put forward the classification of AEP superfamily into three major clades, namely, AEP proper clade, NCLDV/Herpesvirus primase clade and PrimPol clade ([4](#)). Mimiviral gene product of L537, gp577, which is annotated as a hypothetical protein in the NCBI database was classified as part of the NCLDV/Herpesvirus primase clade—structurally composed of a conserved C-terminal β-strand-rich region that has three conserved cysteines and a histidine residue ([4](#)). Our thorough sequence analysis and phylogeny suggested gp577 to be a PrimPol. Purified gp577 is a homodimer and its biochemical characterization demonstrated that it is a PrimPol with terminal transferase and translesion synthesis activities. Additionally, we provide evidence for gp577's reverse transcriptase activity and its ability to utilize a variety of substrates. To the best of our knowledge, gp577 is the first PrimPol to be identified and characterized in an NCLDV.

MATERIALS AND METHODS

Sequence analysis of gp577

To generate sequence alignment and phylogeny, distantly related proteins were identified by PSI-BLAST against NCBI non-redundant database using gp577 as a query sequence. Sequences that showed at least 30% identity with gp577 were selected. Some well-characterized AEPs such as PriS of *Sulfolobus solfataricus,* p41 of *Pyrococcus furiosus,* PRI1 of *Saccharomyces cerevisiae* and PrimPols such as pRN1 plasmid encoded ORF904 of *Sulfolobus islandicus* and human PrimPol were also taken as seed sequences for the iterative BLAST with an e-value threshold of 0.0001. Another characterized protein, namely, PrimPol-like protein (PPL1) of *Trypanosoma brucei* was also added to the alignment manually. Sequences retrieved were aligned by MUSCLE and the phylogenetic tree was constructed using Maximum Likelihood using Jones-Thornton Taylor (JTT) as substitution model and 1000 bootstrap replicates with default parameters in MEGA 7.0 ([25](#)).

Cloning of L537 gene and construction of gp577 mutants

L537 gene was amplified from mimivirus genomic DNA and cloned in pET28a expression vector at SacI and XhoI restriction enzyme sites. The critical residue in each of the three putative primase motifs identified (motif I - **D**FD$_{92-94}$ or **D**ID$_{151-153}$, motif II – SK$\underline{\textbf{H}}_{171-173}$, motif III – V$\underline{\textbf{D}}_{212-213}$ or F**D**$_{238-239}$) were mutated to alanine by site-directed mutagenesis. There were two possibilities for motif I, DFD$_{92-94}$ or DID$_{151-153}$, and in order to identify the correct motif I, the first aspartate of both motifs (D92 and D151) were mutated to alanine. Similarly, for motif III, two aspartates (D213 and D239) were mutated to alanine. The parental recombinant plasmid was polymerase chain reaction-amplified by using the mutagenic primers (Supplementary Table S1) and XT-20 polymerase (Genei Labs, India). Parental plasmid was digested with DpnI (Thermo Fisher Scientific) and the mutation in L537 gene was confirmed by sequencing (SciGenom Labs, India). *Escherichia coli* DH5α cells were used to maintain the recombinant plasmids of wild-type as well as mutant L537 gene(s) and *E. coli* BL21 (DE3) RIPL cells were used for overexpression of the protein.

Expression and purification of gp577 and its mutants

The wild-type gp577 and its mutants were purified by using the common procedure described below. One liter culture of *E. coli* BL21 (DE3) RIPL cells, transformed with the recombinant plasmid, was grown in the presence of appropriate antibiotics at 37°C in LB broth supplemented with 50 μM ZnCl$_2$. At an optical density of 0.7, expression of gp577 was induced by the addition of 0.2 mM isopropyl-β-D-thiogalactopyranoside and cells were further incubated at 16°C for 16 h. Cells were harvested by centrifugation, resuspended in Buffer A [50 mM Tris–HCl (pH 7.4), 20 mM imidazole, 500 mM NaCl, 10% glycerol, 1 mM phenylmethylsulfonyl fluoride (PMSF) and 1 mM benzamidine hydrochloride] and lysed by ultra-sonication. Upon centrifugation at 12 500 *g*, the cell-free extract containing the soluble gp577 protein was loaded onto a pre-equilibrated 1 ml Hi-Trap column (GE Healthcare) and the protein was eluted using a 100–600 mM imidazole gradient. Peak fractions were further purified using HiLoad 16/600 Superdex 200 pg column (GE Healthcare) equilibrated with Buffer B [50 mM Tris–HCl (pH 8.0), 500 mM NaCl and 5% glycerol]. To determine protein purity, the eluted fractions were subjected to 12% sodium dodecylsulphate-polyacrylamide gel electrophoresis (SDS-PAGE) analysis. Pure fractions were pooled, concentrated to approximately 0.5 mg/ml using vivaspin turbo centrifugal concentrators and stored as aliquots at −80°C. The concentration was determined by Bradford's method of estimation using bovine serum albumin as the standard protein. Dimeric nature of the purified proteins was confirmed by gel filtration chromatography using a Sephacryl S-200 HR column (GE Healthcare).

Primer synthesis assays

Coupled primase-pyrophosphatase assay. Pyrophosphate (PPi) released upon the incorporation of nucleoside monophosphate (NMP) into the RNA primer was cleaved using commercially available pyrophosphatase to produce

inorganic phosphate (Pi). Malachite green reagent forms a green colored complex with the released Pi that was estimated spectrophotometrically (26). Reaction mixture (30 μl) containing 2 nM of ΦX174 circular single-stranded virion DNA (New England Biolabs) as template, 80 μM of each of the four NTPs (Promega), 5 mM MgCl$_2$, 0.1 Unit of pyrophosphatase (Sigma-Aldrich) and 500 nM gp577 was incubated at 30°C for 30 min. Reaction was stopped by the addition of 50 mM ethylenediaminetetraacetic acid (EDTA), and the volume was made up to 800 μl using MilliQ water. Two hundred microliters of the freshly prepared malachite green reagent (27) was added and incubated at room temperature (∼25°C) for another 30 min, and the absorbance was measured at 620 nm. A phosphate standard curve was constructed by taking known concentrations of potassium dihydrogen phosphate in the range of 1 to 10 μM. Control reaction lacked the purified enzyme.

Fluorescence primase assay. PicoGreen, a cyanine dye, has higher binding affinity for dsDNA over ssDNA (28–30). This property of PicoGreen was used to monitor the formation of RNA primer on circular and linear single-stranded DNA templates. Reaction mixture (30 μl) containing different templates, ΦX174 or M13 circular single-stranded virion DNA (2 nM) or 34-mer blocked at the 3′ end with dideoxycytidine (100 nM), 80 μM of each of the four NTPs, 5 mM MgCl$_2$ and 500 nM gp577 were incubated at 30°C for 5 min and the reaction was stopped by adding 50 mM EDTA. A 50-μl aliquot (1:200 diluted in TE buffer) of PicoGreen dye (Thermo Fisher Scientific) was added and incubated at room temperature for 5 min. Fluorescence spectra were recorded on a spectrofluorometer (JASCO FP-8300) at an excitation wavelength of 490 nm and an emission wavelength between 500 and 600 nm. A control reaction without the enzyme was setup for each of the three templates.

Gel-based primer synthesis assay. Reaction mixtures (10 μl each) containing template [0.5 μg ΦX174 or M13 circular single-stranded virion DNA or 50 nM of 34-mer blocked template (Sequence 14, Supplementary Table S1), 5 mM MgCl$_2$ or 1 mM MnCl$_2$, 200 nM gp577 or its mutants with buffer P (10 mM Tris–HCl and 1 mM dithiothreitol (DTT) and either 80 μM of each of the four NTPs and [α-^{32}P] ATP (50 nM; ∼1800 Ci/mmol, Board of Radiation and Isotope Technology, Hyderabad, India) or 80 μM of each of the four dNTPs (Thermo Fisher Scientific) and [α-^{32}P] dATP (50 nM; ∼3500 Ci/mmol) were set up to monitor RNA and DNA primer synthesis, respectively. Reaction mixtures were incubated at 30°C for 30 min and terminated by adding EDTA to a final concentration of 50 mM. 2X Gel loading dye (80% formamide, 20 mM EDTA, 1 mg/ml bromophenol blue and 1 mg/ml xylene cyanol) was added to the reaction mixtures and heated at 95°C for 5 min, and the products were separated on a 20% denaturing PAGE (7 M urea) and visualized by autoradiography using Storm 825 or Typhoon FLA 9500 phosphorimager (GE Healthcare).

Terminal transferase assay

To check the terminal transferase activity of gp577, a random 15-mer oligonucleotide (Sequence 15, Supplementary

Table S1) was 5′ end labeled with [γ-^{32}P] ATP (∼3500 Ci/mmol, Board of Radiation and Isotope Technology, Hyderabad, India). Extension of this labeled substrate with NTPs and dNTPs was monitored in separate reactions (10 μl) containing buffer P, 50 nM DNA substrate, 5 mM MgCl$_2$, 100 nM gp577 and either 80 μM of NTPs or dNTPs. Similarly, two 34-mer oligonucleotides with the same sequence, one unblocked (Sequence 13, Supplementary Table S1) and the other blocked (Sequence 14, Supplementary Table S1) at the 3′ end with ddCTP, were 5′ end labeled. The presence of ddCTP at the 3′ end does not allow extension and this substrate serves as a control (10). Reaction mixtures were incubated at 30°C for 5 min and terminated by adding 50 mM EDTA. Further, 20-mer homo-oligomeric poly(dA) and poly(dT) ssDNA sequences were used to confirm template independent extension by gp577 (10). Similarly, ability to extend the 3′ end of a blunt ds-DNA was checked by annealing a 5′ labeled 20-mer poly(T) to a 20-mer poly(A) oligonucleotide (Supplementary Table S1, Sequence 21 annealed to sequence 22). Reactions were composed of buffer P, 50 nM DNA substrate (either one of the two homo-oligomers or the dsDNA), 80 μM of NTPs or dNTPs, 1 mM MnCl$_2$ and 500 nM gp577. Upon incubation at 30°C for 30 min, reactions were terminated with 50 mM EDTA. Products were separated and visualized as described for primase assay.

Primer extension assays

A 15-mer DNA (sequence 15, Supplementary Table S1) or RNA (sequence 24, Supplementary Table S1) primer labeled with [γ-^{32}P] ATP at its 5′ end annealed to a 34-mer DNA (sequence 14, Supplementary Table S1) or 34-mer RNA (sequence 23, Supplementary Table S1) template was used to test the primer extension function of gp577 and its mutants. Reactions (10 μl) containing buffer P, different combinations of 50 nM primer-template DNA/RNA, 5 mM MgCl$_2$ or 1 mM MnCl$_2$, 100 nM gp577 mutants or specified concentration of the wild-type enzyme and 80 μM of NTPs or dNTPs were incubated at 30°C for 5 min. Single nucleotide incorporation assays were performed in the presence of 50 nM primer-template DNA, 5 mM MgCl$_2$ or 1 mM MnCl$_2$ and varying concentrations (0.1–20 μM) of NTPs or dNTPs. Reactions were incubated at 30°C for 5 min, terminated, resolved and visualized as described previously.

Translesion DNA synthesis assays

For the standing-start experiment, a 15-mer primer (Sequence 16, Supplementary Table S1) labeled at its 5′ end with [γ-^{32}P] ATP was annealed to an unmodified 50-mer control template (Sequence 18, Supplementary Table S1) or to the same 50-mer with either N^2-Benzyl deoxyguanosine (N^2-Bn-dG) (Sequence 19, Supplementary Table S1) (31) or 8-oxo-deoxyguanosine (8-oxo-dG) modification (sequence 20, Supplementary Table S1) at the 16th position from the 3′ end. Single nucleotide incorporation assays (10 μl) were performed in the presence of buffer P, 50 nM primer-template DNA, NTPs or dNTPs (varying concentrations from 0.1 to 20 μM) and 1 mM MnCl$_2$. For running-

start experiment, an 11-mer primer (Sequence 17, Supplementary Table S1) labeled at its 5′ end was annealed to the unmodified 50-mer or one of the two modified 50-mer templates. Both standing-start and running-start reactions were incubated at 30°C for 5 min or the indicated time, terminated and then visualized as described previously.

RESULTS

gp577 of mimivirus is a putative PrimPol

Product of mimiviral gene L537 was annotated as a hypothetical protein (gp577) in the NCBI database and classified as a putative member of the AEP superfamily (4). A PSI-BLAST search of gp577 retrieved similar hypothetical proteins from other megaviruses such as *Acanthamoeba castellanii* mamavirus (AEQ61009.1), Powai lake megavirus (ANB50755.1), hirudovirus strain Sangsue (AHA45034.1), Saudi moumouvirus (AQN68474.1), megavirus courdo11 (AFX92739.1), etc. gp577 appears to be present only in some mimiviruses described in the lineages A, B or C as the iterative BLAST search failed to retrieve similar proteins of non-mimiviral origin. A phylogenetic tree of family B DNA polymerase from representative members of the NCLDV family confirmed this observation and suggested that gp577 was probably acquired by the group I members of *Mimiviridae* family (Figure 1A). A second protein from mimivirus (gp857, product of L794 gene and accession number YP_003987326.1) was also retrieved. gp857 showed 39% identity with gp577 of mimivirus suggesting it to be a paralog and is present only in some mimiviruses.

An alignment of gp577-like hypothetical proteins of mimiviruses with PrimPols of archaea and eukaryotes, including well-characterized proteins such as ORF904 of pRN1 plasmid from the crenarchaeote *Sulfolobus islandicus* (7), human PrimPol CCDC111 (5) and PPL1 protein of *Trypanosoma brucei* (6) is shown in Figure 1B. The related archaeo-eukaryotic primase (AEP) family members such as p41 protein of *Pyrococcus furiosus* (32), PriS of *Sulfolobus solfataricus* (7) and PRI1 of *Saccharomyces cerevisiae* (33) have also been aligned (Figure 1B). Sequence alignment helped in identifying the conserved primase motifs I (DFD_{92-94}), II ($SKH_{171-173}$) and III ($VD_{212-213}$) in mimiviral PrimPol. The Zn finger (ZnF) motif (CHCC) is located after motif III in the well-characterized PrimPols and mimiviral PrimPol, while it is sandwiched between motifs I and II in primases from the proper AEP-clade (Figure 1B). Further, a phylogeny generated with AEP-proper clade proteins and PrimPols suggested gp577 to be a probable PrimPol (Figure 1C), although sequence identity of gp577 with these proteins is <40% (Figure 1B).

gp577 is a homodimeric protein

L537 gene of mimivirus was amplified and engineered into the T7 vector, pET28a for overexpression in *E. coli*. Of the various *E. coli* expression strains tested, *E. coli* BL21 (DE3) RIPL cells showed detectable expression levels. Protein was purified by affinity and size exclusion chromatographies. Protein fractionated predominantly as a dimer during size exclusion chromatography when using 16/600 Superdex-200 pg column, which was further confirmed by separating the purified protein on a Sephacryl S-200 HR column (Supplementary Figure S1A). Purified protein was subjected to SDS-PAGE analysis to verify its purity (Figure 2A, lane 1). Inclusion of $ZnCl_2$ in the growth medium resulted in enhanced primase activity of the purified gp577 (data not shown).

gp577 catalyzes *de novo* RNA and DNA primer synthesis

De novo primase activity of gp577 was demonstrated by the coupled primase-pyrophosphatase assay (26) using ΦX174 circular ssDNA as template. No primase activity was detected in the control reaction where gp577 was not added (Figure 2B). The primase activity of gp577 was also verified by a fluorescence-based assay using PicoGreen dye. Detectable level of primase activity was observed at gp577 concentrations of 200 nM and above, whereas no primase activity was detected in the reaction devoid of the purified enzyme (Supplementary Figure S1B). The enzyme was found to be capable of performing *de novo* RNA synthesis on two naturally occurring ssDNA templates (ΦX174 and M13mp18 virion DNA) as well as a synthetic, linear 34-mer ssDNA (Figure 2C). gp577's ability to form primers was further confirmed by gel-based primer synthesis using the same templates used for the fluorescence-based assay (Figure 2D, lanes 2, 4 and 6). Furthermore, we also investigated if gp577 could utilize dNTPs for primer synthesis as such activity is found to be associated with several AEPs (5,7,10). gp577 was able to produce DNA primers on the linear 34-mer ss-DNA but only at nearly double the enzyme concentration to that used for RNA primer synthesis (Figure 2E, lanes 2–6). Replacing the co-factor magnesium with manganese considerably improved the DNA primer synthesis with as low as 0.1 mM Mn^{2+} supporting *de novo* DNA synthesis (Figure 2F, lane 2). Absence of the cofactor from the reaction mixture prevented the formation of DNA primers (Figure 2F, lane 1). Similar to RNA primer synthesis, the two circular DNAs supported synthesis of long DNA primers (Figure 2G, lanes 4 and 6). Overall, these results helped identify gp577 as an RNA/DNA primase.

Identification of gp577 primase motifs

Sequence alignment of gp577 with the well-characterized PrimPols helped in identifying the motifs I (DFD_{92-94}), II ($SKH_{171-173}$) and III ($VD_{212-213}$) (Figure 1B). Primase motifs I and III bind divalent cation and motif III mediates the nucleophilic attack on the incoming NTP by 3′-hydroxyl group while motif II forms the nucleotide-binding site (33). The first aspartic acid residue of motif I coordinates with aspartic acid of motif III in binding Mg^{2+} or other divalent cations (34,35). There are two possible DxD motifs in gp577: DFD_{92-94} and $DID_{151-153}$. In order to identify the correct motif I, the first aspartic acid residue of both DxD motifs was mutated. Similarly, there are two possibilities for motif III ($VD_{212-213}$) and ($FD_{238-239}$). Thus, four aspartates at positions, 92, 151, 213 and 239; and a key histidine
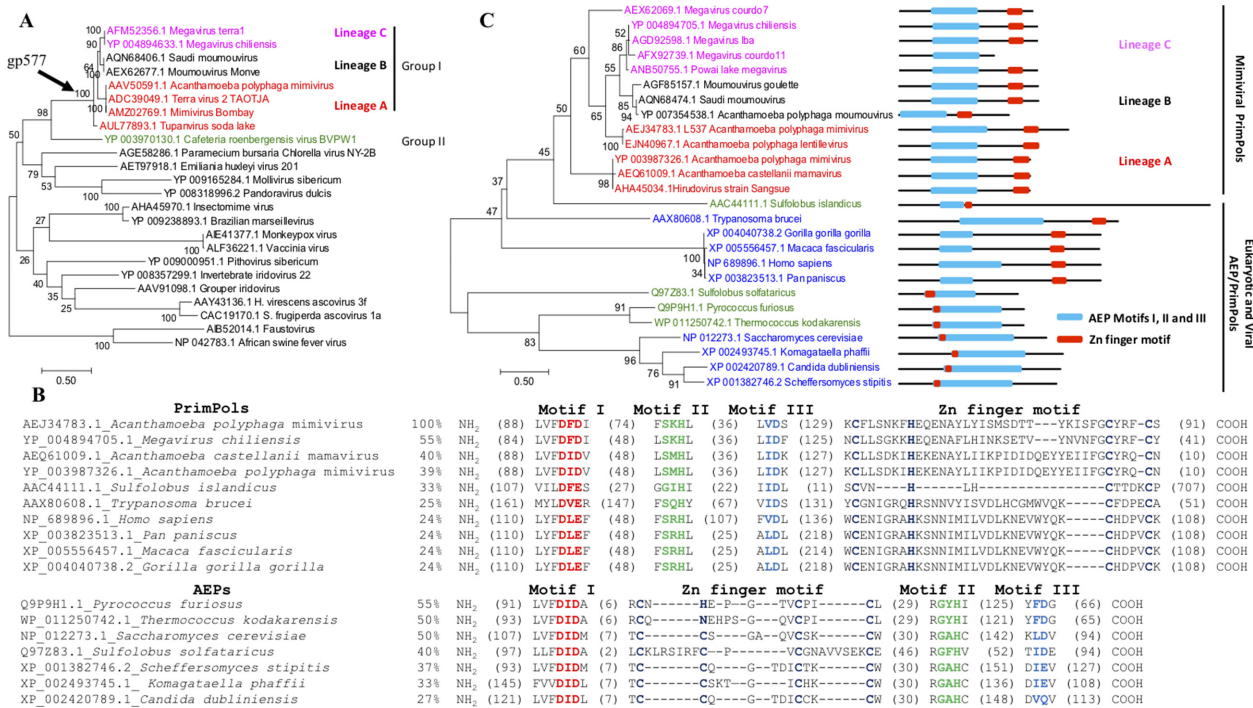
Figure 1. Sequence analysis of gp577. (**A**) Maximum likelihood phylogenetic tree of family B DNA polymerase from NCLDVs. Arrow shows the probable acquisition of gp577 by *Mimiviridae* group I members. Lineages A, B and C of *Mimiviridae* group I are colored in red, black and pink, respectively. *Mimiviridae* group II is colored in green. Scale bar represents number of substitutions per site. (**B**) Multiple sequence alignment of gp577 with mimiviral gp577-like proteins and AEPs from eukaryotes and archaea. Motifs I, II, III and zinc finger motif are shown in red, green, blue and yellow colors, respectively. Proteins are designated by their protein IDs and the species name is separated by an underscore. Alignment obtained from MUSCLE was manually edited and numbers in parenthesis between the motifs indicate the number of amino acids. (**C**) Maximum likelihood phylogenetic tree of mimiviral gp577-like proteins and AEPs. Domain organization of the proteins depicting the position of primase motifs and Zinc finger is also shown. Scale bar represents number of substitutions per site. The length of proteins in domain organization is shown approximately to scale and motifs I–III and zinc finger motif are shown in blue and red, respectively. Colors used: dark blue, eukaryotes; green, archaea.

residue of motif II at position 173 were mutated to alanine and the mutants were purified using the same protocol as wild-type gp577 (Figure 2A, lanes 2–6). Like the wild-type protein, all mutants eluted as dimers during size exclusion chromatography (data not shown).

The putative active site mutants were screened for their RNA and DNA primase activities using the 34-mer ssDNA template. gp577 mutants D92A, H173A and D213A lost the RNA primase activity (Figure 2H, lanes 3, 5 and 6), whereas D151 and D239A could still perform primer synthesis (Figure 2H, lanes 4 and 7). This suggests the role of residues D92, H173 and D213 in primer synthesis and hence, they could potentially form the motif I, II and III, respectively, of gp577 active site. DNA primase activity of gp577 mutants was identical to that observed for RNA synthesis except for the mutant D92A, which failed to synthesize RNA primers but supports DNA primer formation (Figure 2I, lane 3). Thus, the residues D92, H173 and D213 presumably form the catalytic site of gp577 protein.

Interestingly, products of length larger than the template (34-mer ssDNA) were consistently observed during both RNA and DNA primase assays (Figure 2D and G, lane 2). These longer products could potentially be due to terminal transferase activity possessed by gp577. This possibility was systematically explored in subsequent experiments.

Probing gp577's terminal transferase activity

While RNA primers synthesized on ΦX174 and M13 virion DNA templates varied in length (Figure 2D and G, lanes 4 and 6); interestingly, RNA/DNA primers synthesized on the blocked linear 34-mer ssDNA, consistently showed the formation of products longer than 34 nucleotides (Figure 2D and G, lane 2). This could mean that gp577 is extending the newly synthesized primer beyond the template in a template-independent manner. To check the terminal transferase activity, a random 15-mer ssDNA labeled at the 5′ end with $[\gamma\text{-}^{32}P]$ ATP was incubated with gp577 and NTPs or dNTPs. Extension of the substrate DNA with dNTPs and NTPs was observed (Figure 3A, lanes 2 and 4). To confirm the 3′ extension activity of gp577, two substrates, blocked 34-mer and the same 34-mer with an unblocked 3′ end labeled at the 5′ end with $[\gamma\text{-}^{32}P]$ ATP, were used for the assay. Extension was seen with both dNTPs and NTPs only when the unblocked ssDNA was used (Figure 3B, lanes 4 and 8), while the blocked substrate could not be extended (Figure 3B, lanes 2 and 6). This implies either the presence of a terminal transferase activity or extension of the 34-mer substrate in a template-dependent manner based on micro-homologies within the DNA substrate as described previously (36).

To validate the terminal transferase activity, 5′ labeled 20-mer homo-oligomeric sequences were used. As
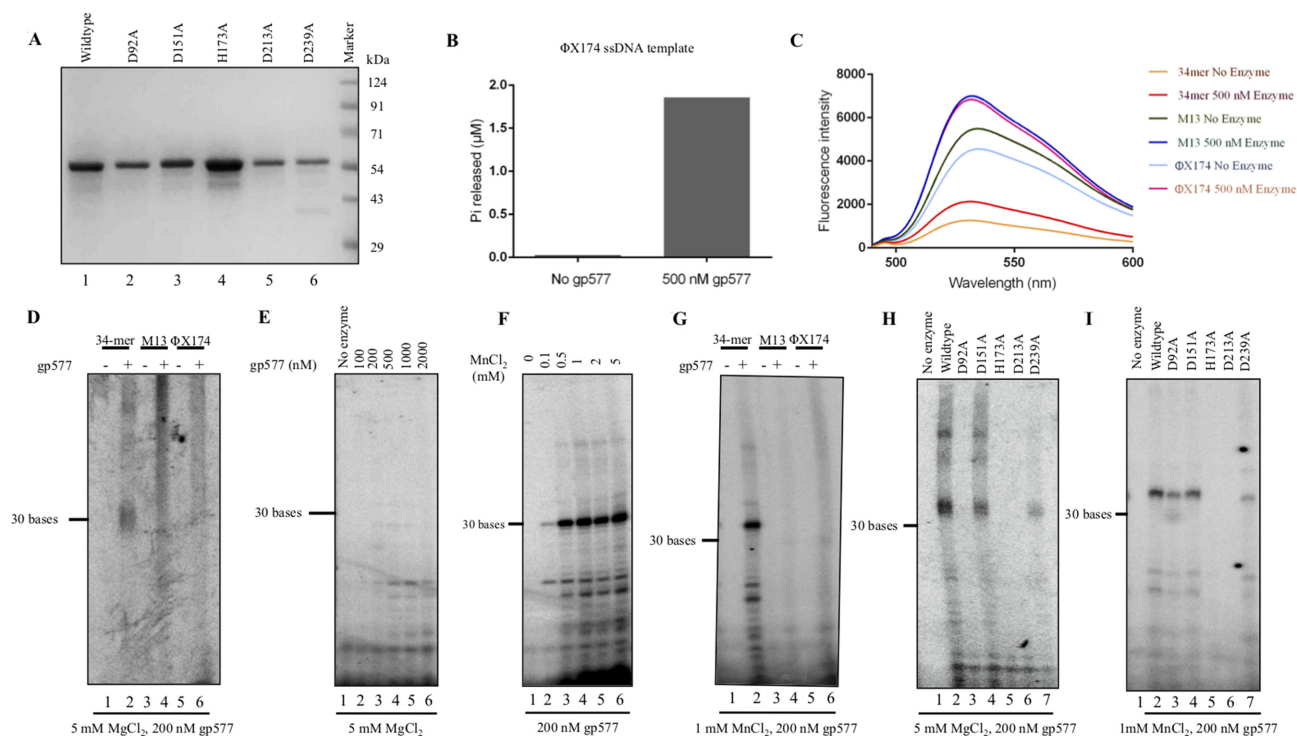
Figure 2. Purified gp577 exhibits RNA/DNA primase activity. (**A**) SDS-polyacrylamide gel analysis of the purified gp577 and its mutants. (**B**) Demonstration of primase activity of gp577 by a coupled primase-pyrophosphatase assay. φX174 circular single-stranded virion DNA (2 nM) was incubated with 80 μM of each NTP, 5 mM $MgCl_2$, 0.1 unit pyrophosphatase and 500 nM gp577 at 30°C for 30 min. Inorganic phosphate released was quantified spectrophotometrically by the addition of malachite green reagent. (**C**) PicoGreen-based primase assay with linear and circular ssDNA. (**D**) Autoradiogram showing the *de novo* addition of NTPs on circular and linear templates by gp577. (**E**) Formation of DNA primers does not occur efficiently with Mg^{2+} as the cofactor even at gp577 concentration of 2000 nM. RNA and DNA synthesis was monitored by incorporation of [α-32P] ATP and [α-32P] dATP, respectively by gp577. (**F**) DNA primase activity with varying concentrations of the cofactor $MnCl_2$, lane 1, no cofactor, lanes 2–6: 0.1, 0.5, 1, 2 and 5 mM $MnCl_2$, respectively. (**G**) *De novo* synthesis of DNA on linear and circular ssDNA. (**H**) Screening of gp577 mutants of putative motifs I, II and III for RNA (H) and DNA (**I**) primase activities. Primase assay was performed using 200 nM of gp577 or its mutants, D92A, D151A, H173A, D213A and D239A.

these sequences cannot form micro-homology based partial double-stranded DNA, they help to distinguish between template-dependent and template-independent nucleotidyl transferase reactions. Incubation of two homo-polymers poly(A) and poly(T) in separate reactions with either NTPs or dNTPs did not produce any extension products (data not shown). However, substituting the co-factor magnesium with manganese produced extension of poly(A) as well as poly(T) substrates. Poly(A) supported significant extension mainly in the presence of all dNTPs or dTTP (Figure 3C, lanes 2 and 4). Extension was also observed with NTPs (Figure 3C, lanes 8–12). Poly(T) substrate showed extensive elongation with all dNTPs except dATP (Figure 3D, lanes 2–6), whereas product formation is seen with all the four NTPs (Figure 3D, lanes 8–12). Presumably, in the presence of only dATP, the enzyme adds dATP in a template-dependent manner (DNA primase activity) rather than extending the poly(T) substrate. gp577 also extended the 3′end of a blunt dsDNA with dNTPs as well as NTPs while displaying a preference for the latter (Figure 3E, lanes 2 and 4). Further, we screened each of the gp577 mutants for their terminal transferase activity. As previously observed for the RNA primase activity, mutants D92A, H173A and D213A showed reduction or complete loss of activity (Figure 3F and G, lanes 3, 5 and 6), whereas D151 and D239A retain the terminal transferase ability (Figure 3F and G, lanes

4 and 7). These results clearly suggest gp577 to possess DNA/RNA terminal transferase activity. Terminal transferase activity of a primase from a large dsDNA virus has not been reported so far, but Hepatitis B virus polymerase, namely, HP, shows this activity (37).

gp577 is a DNA/RNA polymerase

The alignment of gp577 with PrimPols (Figure 1B) prompted us to investigate the DNA polymerase activity of gp577. Radiolabeled 15-mer primer annealed to a blocked 34-mer was used as the template. gp577 extended the primer with dNTPs, and also with NTPs while using magnesium as the cofactor; however, formation of the expected full-length product was minimal (Supplementary Figure S2A). Qualitatively, gp577 always formed much longer products with NTPs as compared to dNTPs under identical reaction conditions (Figure 4A, lanes 2 and 3). The commercially available XT-20 polymerase, used as a control, produced complete extension products with dNTPs owing to its high processivity but fails to utilize NTPs as substrates (Figure 4B, lanes 3 and 6). This confirmed the RNA and DNA polymerase activities to be intrinsic to gp577 and rules out the possibility of contamination of dNTPs with NTPs. When compared to XT-20 polymerase, which extended the primer to 34 bases, gp577 formed products of varying lengths (Fig-
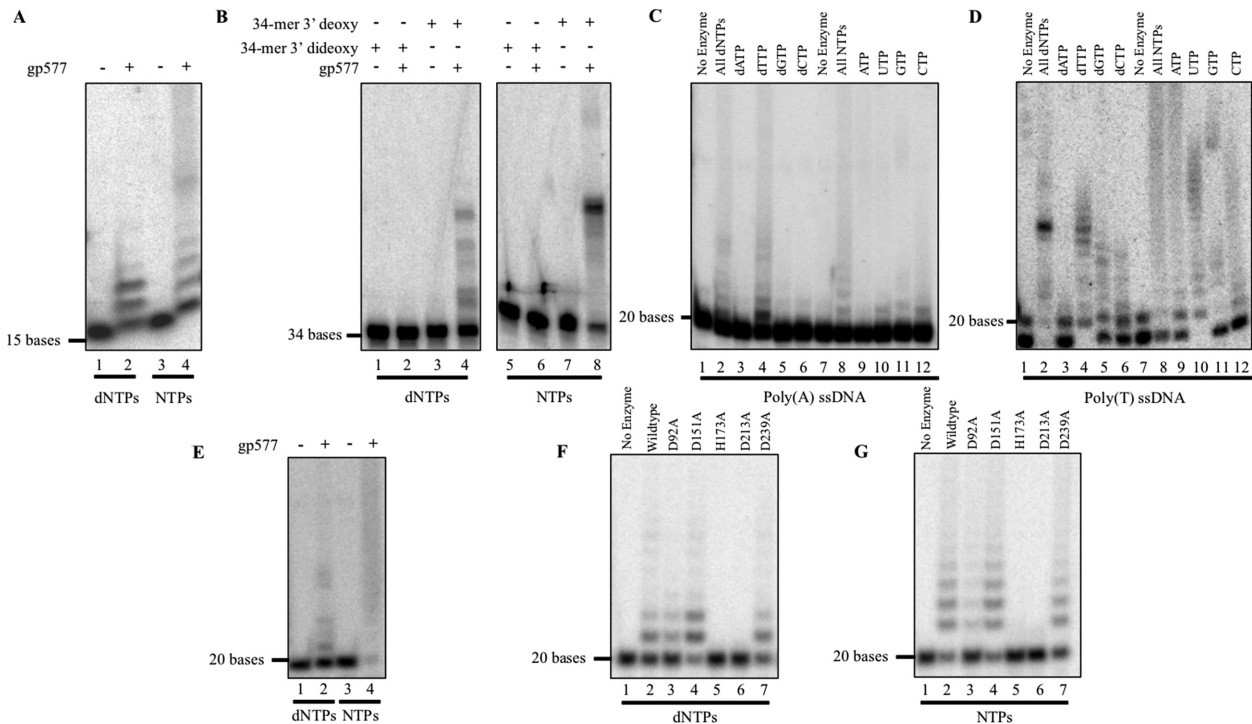
Figure 3. gp577 possesses terminal transferase activity. (**A**) Extension of a ssDNA labeled at the 5′ end with [γ-^{32}P] ATP by 100 nM gp577 using dNTPs and NTPs. (**B**) Terminal transferase activities of gp577 with 5′ [γ-^{32}P] ATP labeled unblocked and blocked templates with NTPs and dNTPs. (**C and D**) Template independent extension of homo-oligomeric sequences by gp577 using dNTPs and NTPs. Reactions with homo-oligomers were carried out using 500 nM gp577, 1 mM Mn^{2+} at 30°C for 30 min. (**E**) Extension of the 3′ end of a blunt dsDNA by gp577. (**F and G**) Probing the terminal transferase activity of gp577 mutants while utilizing dNTPs and NTPs, respectively. About 500 nM gp577 or its mutants and poly(T) as the substrate were used for these reactions.

ure 4B, lanes 2, 3, 5 and 6). Substituting magnesium with manganese led to improved processivity of the enzyme and full-length extension of the primer was observed (Figure 4C and D, lanes 2–6).

As observed earlier during the RNA primase assay, mutants D92A, H173A and D213A displayed much reduced DNA polymerase activity (Figure 4E, lanes 3, 5 and 6), whereas the activities of mutants D151A and D239A were comparable to that of the wild-type protein (Figure 4E, lanes 2, 4 and 7). This observation reiterates the significance of residues D92, H173 and D213 in the active site of gp577. Similar results were obtained when the mutant enzymes were screened for their RNA polymerase activity (Figure 4F). The level of extension for mutants D92A and D213A was greater than that observed during extension with dNTPs (Figure 4F, lanes 2, 3 and 6). This could be possible due to differential affinities of gp577 enzyme toward dNTPs and NTPs as observed earlier (Figure 4A). This intriguing possibility was explored in the experiments that followed.

To further understand the ability of gp577 to utilize dNTPs or NTPs during the polymerase reaction, we performed single nucleotide incorporation assays. Addition of ribo as well as deoxyribonucleotides across the template base, 'dA' was analyzed (Figure 5A) in the presence of either magnesium or manganese as the cofactors. Extension of primer using purine nucleotides was insignificant as more than 95% of the labeled primer remains unextended (Figure 5B, lanes 1–20). Incorporation of the complementary dNTP

occurs in a template-dependent manner as dTTP is inserted mainly against the template adenine forming a '+1' product (about 75%) but incorporation across the second template base, guanine is <10% (Figure 5C, lanes 6–10). While using dNTPs, gp577 probably follows Watson–Crick base pairing pattern, adding mainly the complementary nucleotide and hence, negligible amount (<10%) of dATP, dGTP (Figure 5B, lanes 6–10 and 16–20) or dCTP (Figure 5C, lanes 16–20) is added across the template, adenine. While extending the primer with individual pyrimidine ribonucleotides, gp577 forms several longer products (+1 to +4, at least with 50% extension beyond +1 site) exhibiting non-complementary extension (Figure 5C, lanes 1–5 and 11–15). Identical experiment performed using manganese ions as the cofactor shows extensive formation of the +2 (and even longer, ~50%) products with NTPs (Figure 5D and E, lanes 1–5 and 11–15) as well as with dNTPs (Figure 5D and E, lanes 6–10 and 16–20) hence, displaying low fidelity and template independence.

gp577 can act as a reverse transcriptase

The ability of gp577 to extend a DNA primer-template complex with dNTPs and NTPs compelled us to further investigate the substrate specificity of this enzyme. For this, we tested the extension of three different primer-template combinations viz., RNA primer–DNA template, DNA primer–RNA template and RNA primer–RNA template (Figure 6A–C). gp577 extended the RNA primer annealed to a
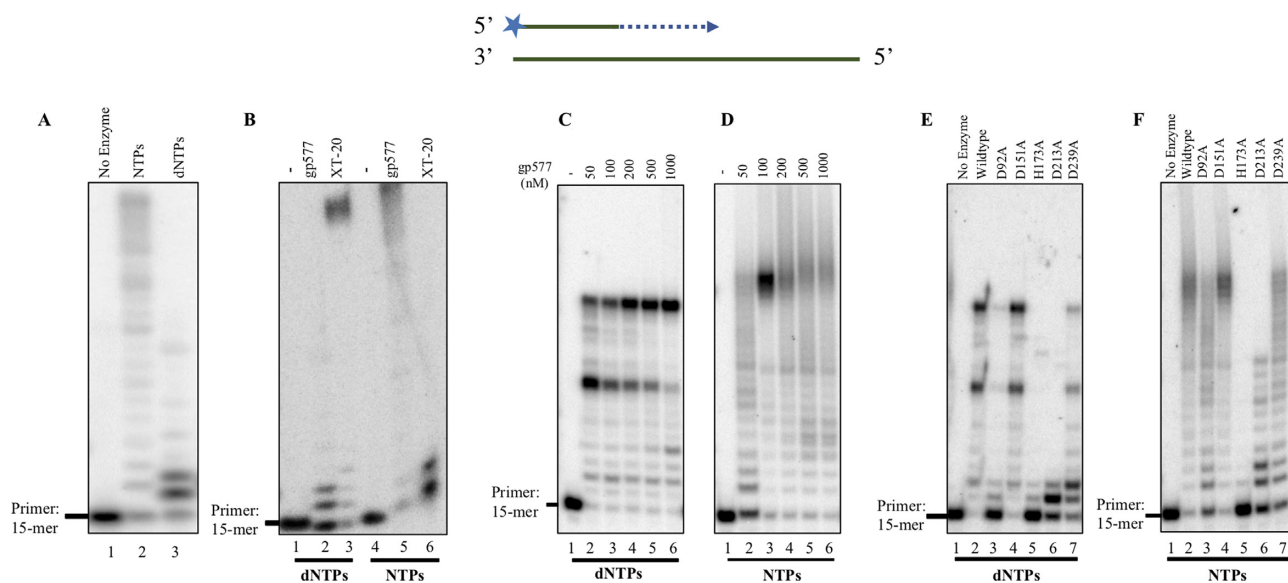
Figure 4. gp577 exhibits DNA/RNA polymerase activity. (**A**) Extension of the annealed DNA primer by NTPs and dNTPs. (**B**) Comparison of the RNA and DNA polymerase activities of gp577 and XT-20 commercial polymerase. (**C** and **D**) Complete extension of primer using dNTPs and NTPs, respectively in the presence of 1 mM Mn^{2+} as the cofactor and varying concentrations of gp577 (Lane 1: No enzyme control, lanes 2–6: 50, 100, 200, 500 and 1000 nM of purified gp577, respectively). The reactions were incubated at 30°C for 5 min. (**E** and **F**) DNA and RNA polymerase assay with gp577 mutants. About 100 nM of the wild-type or mutant enzymes were used for the assay. Mutants D92A, H173A and D213A showed either complete loss or reduction in polymerase activity.

DNA template with dNTPs and NTPs (Figure 6A, lanes 1–5 and 6–10). Additionally, gp577 extended both DNA and RNA primers in a RNA template-dependent manner using dNTPs (Figure 6B and C, lanes 1–5) or NTPs (Figure 6B and C, lanes 1–5) therefore acting as an RNA-dependent DNA polymerase (reverse transcriptase) as well as RNA-dependent RNA polymerase. This observation further underscores the relaxed substrate specificity of the enzyme. Similar to the DNA-dependent polymerase activity, a marked preference for incorporation of NTPs over dNTPs is evident. Also, manganese ions were found to enhance each of the three activities (Supplemental Figure S2B–D). Interestingly, incorporation of dNTPs into the growing DNA chain was profound while extending the RNA primer annealed to DNA (Figure 6A and Supplemental Figure S2B). This could have implications for the *in vivo* role of gp577. Mutants, D92A, H173A and D213A show either partial or complete loss of polymerase activity, whereas mutants D151A and D239A display activity comparable to the wild-type enzyme.

These data collectively suggest gp577 to be a DNA/RNA dependent DNA and RNA polymerase possessing differential affinities and accuracies while utilizing NTPs and dNTPs. In the mimiviral life cycle, significance of such an enzyme possessing diverse substrate specificity remains to be studied.

gp577 is a low fidelity translesion polymerase

The error prone nature of gp577 polymerization and the speculation that TdT activity of archaeal primases might be crucial for translesion synthesis (10) led us to investigate the TLS activity of gp577. The ability of the enzyme to bypass two different modified deoxyguanosines (dG),

an oxidized derivative (8-oxo-dG) and an N^2-benzyl modified dG (N^2-BndG) (Supplementary Figure S3A) was monitored. Running-start experiment, where the modified base was four nucleotides away from the start site (Figure 7A–I) was performed to check the ability of gp577 to bypass a modified base in the template. When gp577 was incubated with an unmodified template-primer, complete extension of the primer was observed while utilizing manganese (Figure 7B, lanes 2–4) as well as magnesium (Supplementary Figure S3B, lanes 2–4) as the cofactor. Upon incubation of gp577 with the template containing N^2-BndG, it was able to bypass the modification forming products beyond the lesion site; however, a strong pause was observed at the modified site with very few products being extended to the complete length of the template (Figure 7C, lanes 2–4). This suggests the ability of gp577 to tolerate the modification and bypass it with low processivity. Similar results were observed with magnesium as the cofactor (Supplementary Figure S3C, lanes 2–4). Bypass of the 8-oxo-dG modified template occurred with lesser efficiency as compared to the N^2-BndG modification (Figure 7D, lanes 2–4 and Supplementary Figure S3D, lanes 2–4).

Further, to assess the fidelity of bypass we performed a single nucleotide insertion (standing start) assay across the modified guanine with varying concentrations of the complementary as well as non-complementary nucleotides (Figure 7A-II). In the presence of magnesium, gp577 bypassed the N^2-BndG modified base, with both the non-complementary (ATP, GTP and UTP) (Supplementary Figure S4A, lanes 1–5, 11–15 and 31–35, respectively) and the complementary (CTP) (Supplemental Figure S4A, lanes 21–25) ribonucleotides. Also, formation of +2 and +3 products (about 40% extension beyond +1 nucleotide) was ob-

5' CAGACGAGCTCATGGCTGA**A**GACAAAATTGAGG**ddC**- 3'
TCT GTT TTAACT CC　**G**- 5'
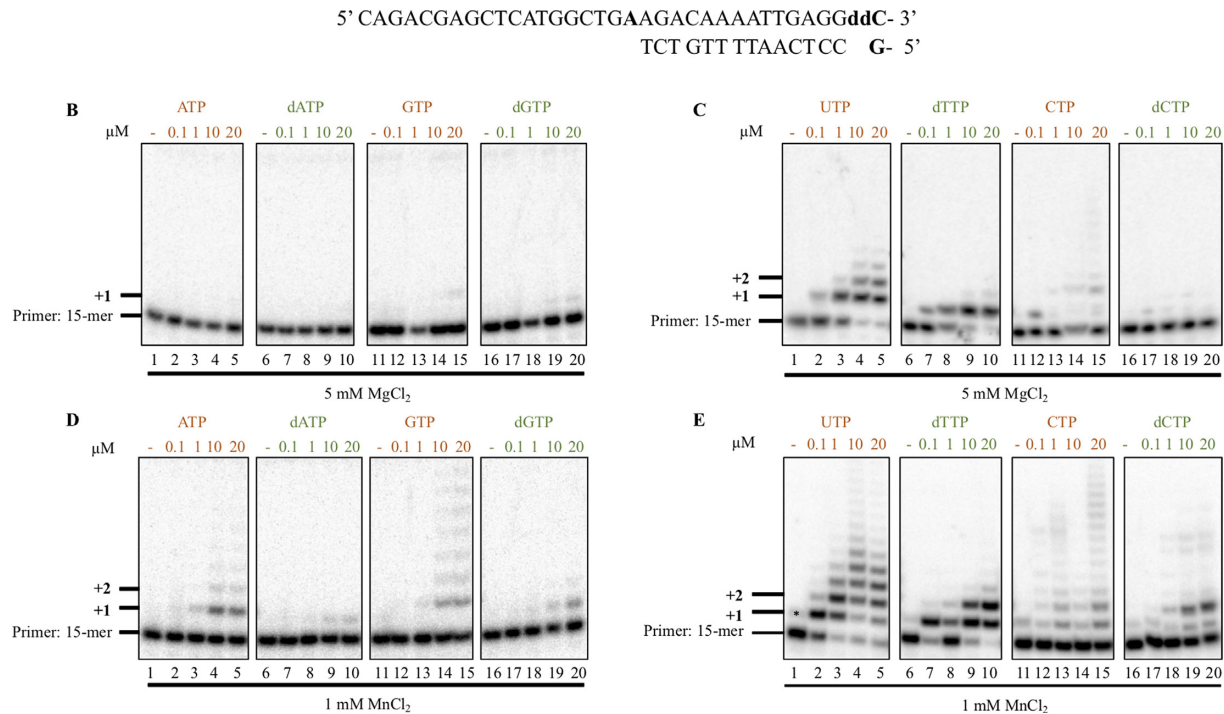
Figure 5. Effect of cofactors on gp577 processivity and fidelity. (**A**) Schematic showing the experimental setup for single nucleotide incorporation assay. (**B** and **C**) Incorporation of varying concentrations of individual NTPs or dNTPs against the templating dA was studied using 5 mM Mg^{2+} as the cofactor. (**D** and **E**) Extension of the 15-mer primer with varying concentrations of NTPs or dNTPs using 1 mM Mn^{2+} as the cofactor. Reactions were performed with 100 nM gp577 enzyme and incubated at 30°C for 5 min.

served thereby reaffirming the low template dependence of this enzyme while utilizing NTPs (Supplementary Figure S4A, lanes 11–15, 21–25 and 31–35). The N^2-BndG base bypass with dNTPs occurred strictly with the complementary (dCTP) nucleotide only (Supplementary Figure S4A, lanes 26–30) and no product formation was observed with the non-complementary (dATP, dGTP and dTTP) nucleotides (about 85% primer remains unextended) (Supplementary Figure S4A, lanes 6–10, 16–20, and 36–40). These results together confirm gp577's ability to bypass the N^2-BndG modified base in the template strand. Bypass with manganese as the cofactor produced extensions beyond the modified site with both NTPs and dNTPs (Figure 7E). Except dATP, all other nucleotides could be used to bypass the N^2-BndG modification (Figure 7E, lanes 1–26). These results clearly indicate that the higher activity promoted by manganese compromises the fidelity of the enzyme. Bypass of the 8-oxo-dG modification by gp577 was inefficient with magnesium using any of the provided nucleotides except ATP (Supplementary Figure S4A, lanes 1–5). In the presence of manganese, extension was observed with ATP, GTP and CTP (Figure 7F, lanes 1–4, 8–10, and 14–17, respectively) while the corresponding dNTPs showed lesser efficiency of bypass (Figure 7F, lanes 5–7, 11–13, and 18–20). Additionally, we also performed standing start assays with a mixture of all four deoxyribonucleotides. Efficient bypass of the N^2-BndG was observed while extension from the 8-oxo-dG was poor (Supplementary Figure S3E–G). Overall, these results suggest the ability of gp577 to tolerate modification in the template DNA and act as a translesion synthesis polymerase.

DISCUSSION

A previous *in silico* study identified gp577 and gp857 (products of L537 and L794 gene, respectively) of mimivirus as putative members of the NCLDV/Herpesvirus primase clade of the AEP superfamily (4). Sequence and phylogenetic analysis corroborated this study and suggested gp577 and gp857 to be potential PrimPols (Figure 1B and C). Alignment of gp577 with well-characterized PrimPols led to the identification of three AEP-like catalytic motifs: I ($DFD_{92–94}$), II ($SKH_{171–173}$) and III ($VD_{212–213}$) and a ZnF motif (CHCC) (Figure 1B). Further, detailed biochemical characterization of the recombinant gp577 protein and mutagenesis of the key catalytic residues confirmed its identity as a bona fide PrimPol—the first PrimPol to be functionally characterized from an NCLDV.

Purified gp577 eluted as a homodimer and is capable of *de novo* RNA and DNA primer synthesis akin to the trypanosomal PPL1 and the human PrimPol, CCDC111 (5,6). Some archaeal primases can start the primer synthesis with both NTPs and dNTPs and have the ability to extend the DNA primer ranging in length from 500 bases up to 7 kb in length (8–12,38), thus behaving like a polymerase. This possibility prompted us to investigate the polymerase activity of gp577. Interestingly, gp577 could extend a DNA primer using dNTPs as well as NTPs with longer products being observed with the latter (Figure 4A). Single nucleotide incorporation assays demonstrated the RNA polymerase activity to be highly error-prone contrary to the DNA polymerase activity, which followed the canonical base-pairing pattern (Figure 5B).
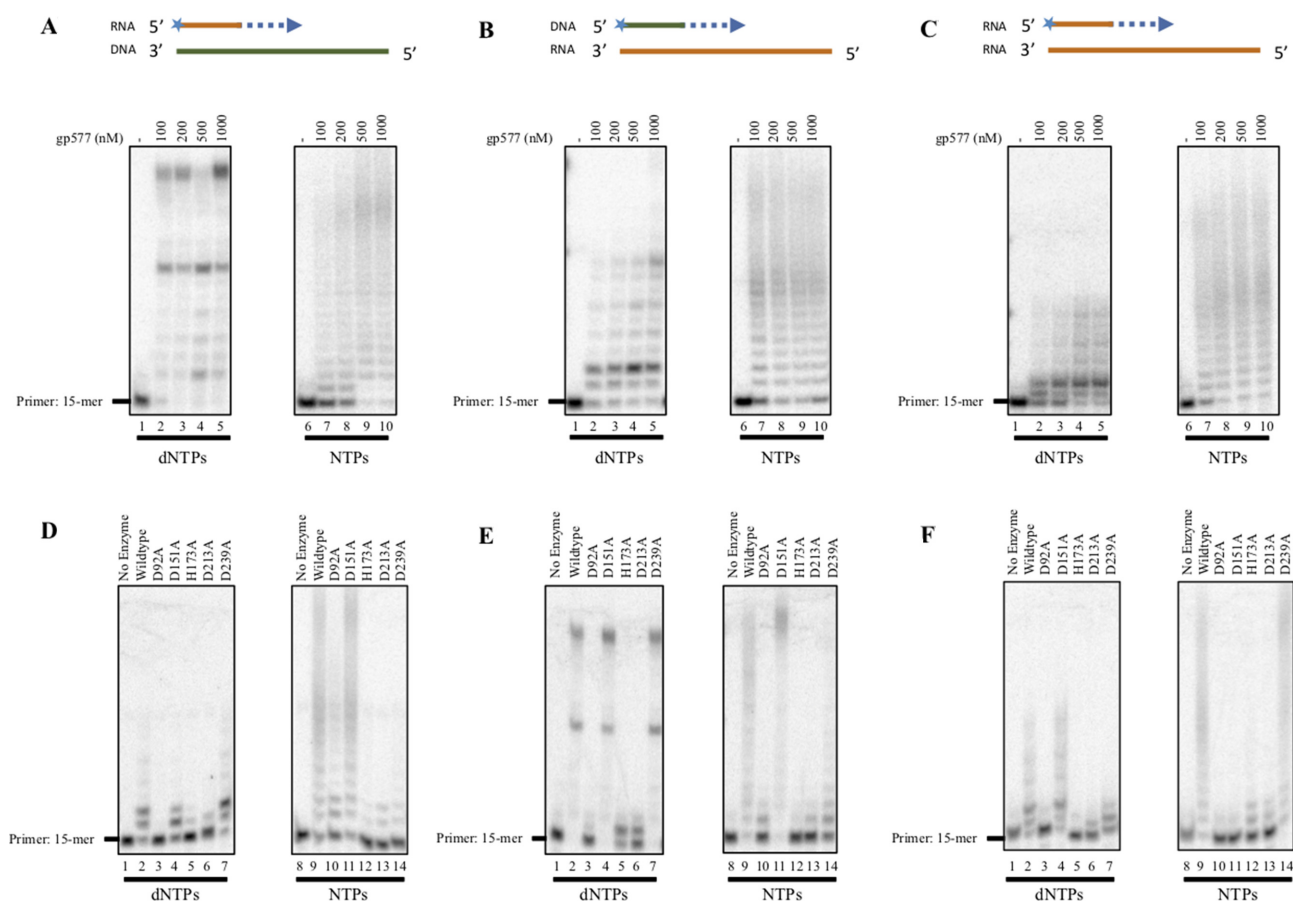
Figure 6. gp577 demonstrates relaxed substrate specificity. (**A**) DNA template-dependent extension of a RNA primer with dNTPs and NTPs mediated by gp577. (**B**) gp577 incorporates dNTPs as well as NTPs while extending a DNA primer annealed to a RNA template. (**C**) Extension of a RNA primer in a RNA template-dependent manner by gp577 using dNTPs and NTPs. All assays were performed using 100 nM of wild-type gp577 with 1 mM $MnCl_2$ and incubated at 30°C for 5 min. (**D–F**) Screening of gp577 mutants for their ability to extend the three different primer-template combinations using dNTPs and NTPs. About 100 nM of each mutant was used for this assay in the presence of 1 mM Mn^{2+} as the cofactor.

Primases belonging to the AEP superfamily possess three conserved motifs. Acidic residues forming motifs I and III are involved in divalent metal binding while motif II is essential for binding the nucleotide (35). As expected, the primase and polymerase activity of gp577 was supported by divalent cations Mg^{2+} and Mn^{2+} with the latter triggering higher activity, *in vitro*. DNA primase activity was especially boosted by the presence of Mn^{2+} (Figure 2E and F). However, the enhanced activity displayed in the presence of manganese compromised the fidelity of synthesis by promoting mis-incorporations during extension of the DNA primer (Figure 5D and E). Manganese induced infidelity has been widely reported for different polymerases (39). Some specialized polymerases preferentially utilize manganese even in the presence of molar excess of magnesium ions (40). The *in vivo* concentrations of this metal cofactor could possibly balance the improved activity while still retaining the desired fidelity (39). Contrary to Mn^{2+}, presence of Mg^{2+} led to decreased processivity but higher fidelity; displayed by extension of the primer in a strictly template-dependent manner (Figures 4A and 5D,E). Mutating the catalytic residues involved in cofactor or nucleotide binding either decreased or completely abolished both the pri-

mase (Figure 2H and I) and polymerase (Figure 4E and F) activities. Interestingly, gp577 displays remarkable substrate tolerance as it can utilize DNA as well as RNA templates for its DNA/RNA polymerase activities thereby acting as a DNA-dependent DNA/RNA polymerase as well as a RNA-dependent DNA/RNA polymerase (Figure 6A–C).

In addition to the primase and polymerase activities, gp577 adds NTPs and dNTPs to ssDNA and blunt-ended dsDNA in a template independent-manner demonstrating its terminal transferase activity (Figure 3A–C). TdT belongs to the family X of DNA polymerases, members of which such as pol λ and pol μ are implicated in DNA damage tolerance via TLS (41,42). Some archaeal AEPs also possess the TdT activity (10,20–21). In bacteria, such as *Mycobacterium tuberculosis*, the AEP domain of LigD protein exhibits TdT activity. Ku-LigD fusion protein is involved in DNA repair by non-homologous end-joining (NHEJ) (43,44). Examples of viral enzymes possessing TdT activity are limited and include the Hepatitis B virus polymerase (HP) (37) and RNA-dependent RNA polymerase enzymes from viruses of the *Flaviviridae* family (45). Mutations of the key catalytic residues of motifs I, II and III of gp577 that constitute the catalytic triad for primase and
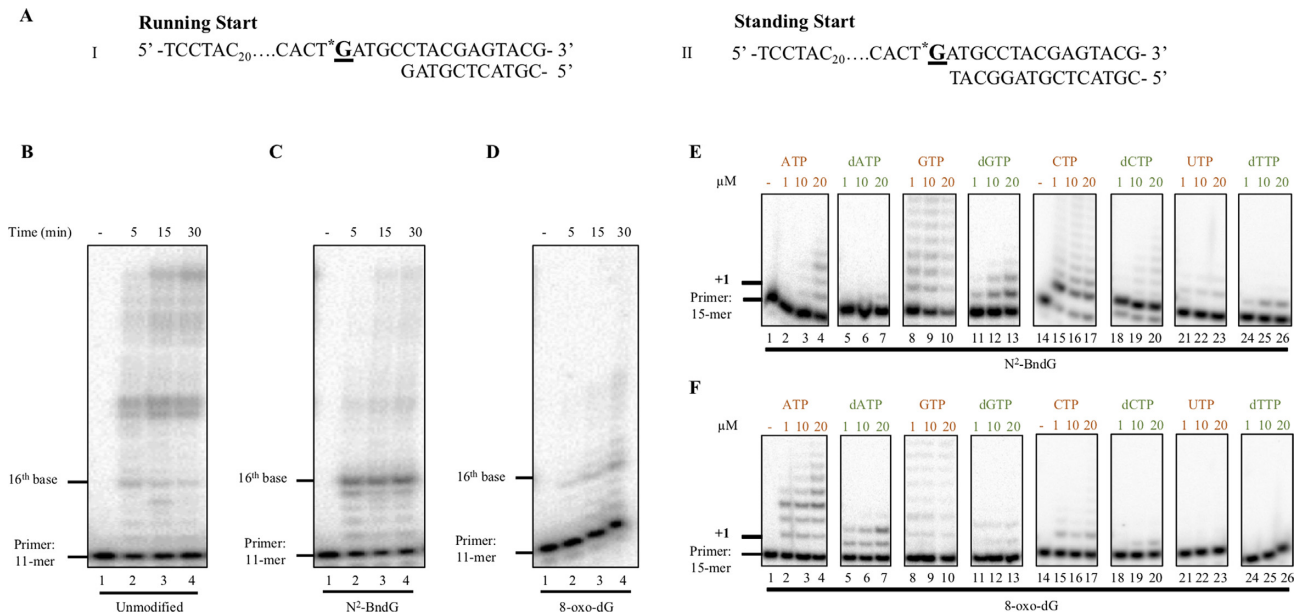
Figure 7. Translesion synthesis activity of gp577. (**A**) A schematic representation of the standing start and running start assay templates used to assess the translesion synthesis ability of gp577. * indicates the modified template guanosine base. Running start polymerization by gp577 on unmodified (**B**), N^2-Bn-dG modified (**C**) or 8-oxo-dG modified (**D**) templates. The reactions were incubated with 100 nM gp577 enzyme at 30°C for 5, 15 or 30 min. Single nucleotide incorporation against the modified template shown in Figure 7A II using the N^2-Bn-dG-modified template, in the presence of 1 mM Mn^{2+} (**E**) or 8-oxo-dG-modified template, in the presence of 1 mM Mn^{2+} (**F**). All single nucleotide incorporation assays were performed with 100 nM gp577 enzyme at 30°C for 5 min.

polymerase activities showed the loss of terminal transferase activity as well thereby confirming the involvement of the same active site in all the three functions (Figure 3B and C).

PrimPols from *Archaeoglobus fulgidus* and *Pyrococcus furiosus* display DNA damage tolerance activity (12). DNA damage tolerance activity of human PrimPol has also been extensively studied (5,17,46). We therefore tested gp577's potential to circumvent lesions in a template DNA. gp577 bypassed the template containing a N^2-Bn-dG adduct as well as an 8-oxo-dG modification. Presence of the modified base lowered the processivity of the enzyme thereby inhibiting formation of the full-length products (Figure 7B–D). Remarkably, gp577 incorporated dNTPs as well as NTPs across the template lesion with greater bypass being observed while utilizing NTPs (Figure 7E and F). The ability to misincorporate NTPs against a damaged template has been documented for translesion synthesis polymerases like pol λ, pol η, pol μ and pol β (47–52). However, contradictory to gp577, these eukaryotic enzymes display a marked preference for dNTPs over NTPs. The intracellular NTP concentration is several fold higher than that of dNTPs (53), and incorporation of NTPs across the lesion is highly probable, *in vivo*. This unique ability of gp577 could possibly serve the dual role of bypassing the lesion with low fidelity while simultaneously 'flagging' the newly formed strand by inserting NTPs, allowing prompt recognition and subsequent removal by DNA repair enzymes.

Mimivirus replication, from infection to release of virus particles, takes about 12 h (54). A rapid increase in the total DNA is observed in the infected cell between 3 and 8 h post-infection (p.i.) that coincides with the highest levels of expression of the putative family B DNA polymerase gene R322 as well as the PrimPol gene, L537 (http://www.igs.cnrs-mrs.fr/Mimivirus/data.html) (24). Owing to its phagosomal mode of entry, mimiviral genomic DNA is susceptible to oxidative damage, which could be tolerated using gp577. In addition to gp577, mimivirus also encodes a family X polymerase (gp347; product of L318 gene) and a DNA mismatch repair enzyme, MutS-like protein (L359) that are also expressed optimally between 3 and 6 h p.i. (24). In addition, mimivirus genome encodes several enzymes involved in the base excision repair (24,55–56). Thus, mimivirus appears to possess a robust DNA repair machinery to correct errors encountered during the replication of its 1.2 Mb genome. It has now been established that mimivirus genome replication takes place entirely in the cytoplasmic viral factories (54,57) where they probably have limited access to host DNA repair enzymes. In addition to gp577, mimivirus also encodes gp857, another putative PrimPol; two primases, gp8 and gp1; as well as an AEP primase-helicase fusion protein, gp229 (24,55–56). DNA content of the mimivirus-infected amoebae increases exponentially during the first 6 to 8 h with an estimated doubling time of 2.7 h (54). Considering the large burst size of mimiviruses (>300 particles per cell) and the large genome, it is quite conceivable that mimiviral genome might possess multiple replication initiation sites as suggested earlier (4). The presence of several primases to initiate replication at multiple sites on the genome or different primases for the leading and lagging strand synthesis and the readily available repair enzymes could be advantageous to mimivirus DNA replication and repair.
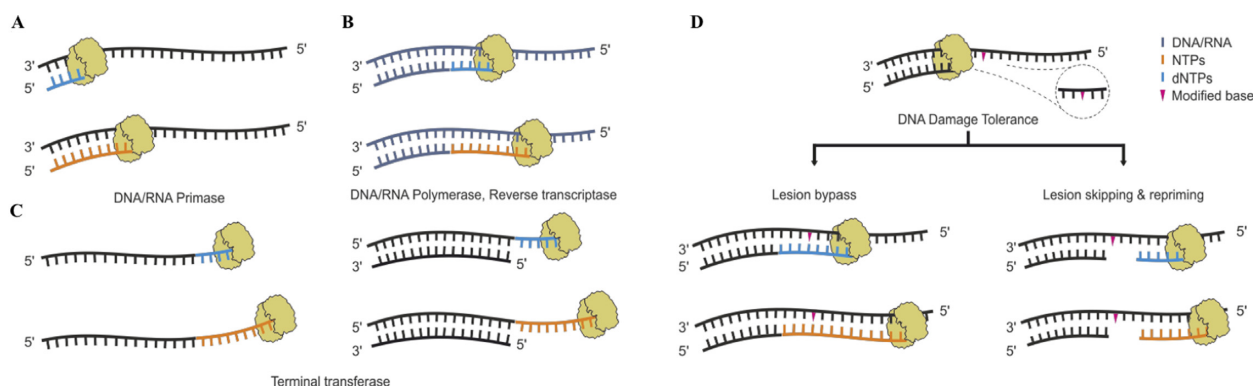
Figure 8. Biochemical activities of gp577 and their probable *in vivo* roles. gp577 can utilize different DNA substrates viz. ssDNA, a primer-template complex or a dsDNA. The enzyme displays varied activities such as DNA/RNA primase (**A**), DNA/RNA-polymerase (PrimPol), reverse transcriptase (**B**) and terminal transferase (**C**). Interestingly, gp577 prefers to utilize NTPs over dNTPs shown by longer product formation while using the former. (**D**) Probable mechanisms utilized by gp577 upon encountering a DNA lesion. Owing to its substrate flexibility, it may utilize either NTPs or dNTPs to directly bypass the lesion (left) thus acting as a translesion synthesis polymerase. Alternatively, gp577 could completely skip the modified base and reprime synthesis downstream of the lesion thereby ensuring continued replication (right). Template (substrate) DNA is shown in black; dark blue indicates either DNA or RNA; sky blue and orange colors indicate the newly synthesized DNA and RNA products respectively, whereas the pink triangle indicates the modified DNA base. The homo-dimeric enzyme is shown in yellow.

Although gp577 is a versatile protein, all the activities associated with it, in general, are error-prone especially while utilizing NTPs as the substrate and manganese as the activating metal ion. Thus, the role of gp577 in conventional replication appears to be unlikely. Alternately, owing to its flexible substrate preference it could primarily act as a DNA damage tolerance enzyme (Figure 8). We speculate that depending on the type of error encountered, gp577 could potentially use two different pathways to help continue DNA replication (Figure 8D). It could act as a translesion synthesis enzyme and bypass the DNA lesion using its TLS activity (Figure 8D, left). It is highly likely that upon bypassing the modified nucleotide, gp577 dissociates from the template allowing other proteins to take over. This mechanism of lesion bypass by gp577 could be similar to the polymerase switch mechanism reported for TLS polymerases (58). Instead, it could completely skip the damaged portion and initiate DNA synthesis downstream of the lesion using its primase activity (Figure 8D, right). Under any of the above circumstances, continued functioning of gp577 could be pro-mutagenic and hence, its functions have to be tightly regulated. It has been recently shown that human PrimPol activities are regulated by its binding to single strand binding proteins (SSBs) (59) and PolDIP2 (polymerase δ-interacting protein 2) (60). These studies are now providing evidence for how the activities of PrimPol are coordinated with the DNA replication machinery in higher eukaryotes. Understanding the regulation of gp577 activities and finding its interacting partners could shed light on its physiological role in mimivirus.

Mimiviral gp577, a multifunctional PrimPol, shares sequence and functional similarities with eukaryotic Prim-Pols. However, the evolutionary history of such a versatile enzyme in mimivirus is mysterious. The eukaryotic Prim-Pols have been predicted to be acquired from a large DNA virus during early evolution and further lost on multiple occasions leading to a patchy phyletic distribution (4). gp577-like protein could have formed a part of the replication machinery of viruses during the transition from an RNA to a DNA world. Replication enzymes of early DNA viruses could have retained the ability to utilize NTPs as a substrate while utilizing DNA/RNA as template, thereby producing a hybrid polymerase enzyme. An ancestral NCLDV containing a gp577-like enzyme possibly served as a source for the eukaryotic PrimPol homologs. However, our sequence and phylogenetic analysis showed presence of gp577-like protein only in group I of *Mimiviridae* family (Figure 1A) thereby suggesting possible loss of this gene by NCLDVs and recent reacquisition by a mimivirus ancestor, perhaps from an eukaryotic host.

In summary, we have identified the first PrimPol in an NCLDV possessing reverse transcriptase, terminal transferase and TLS abilities. The relaxed substrate specificity of this enzyme coupled with the versatile nucleotidyl transferase activities could serve a major role in mimiviral DNA replication and/or DNA damage tolerance pathways. *In vivo* experiments, identifying binding partners and mechanisms of regulation of its activities are needed to decipher the physiological role of gp577 in mimivirus. Furthermore, structural studies of gp577 would help in deducing the coordination of primase, polymerase and terminal transferase activities and the lesion bypass mechanism of gp577.

SUPPLEMENTARY DATA

Supplementary Data are available at NAR Online.

REFERENCES

1. Rattray,A.J. and Strathern,J.N. (2003) Error-prone DNA polymerases: When making a mistake is the only way to get ahead. *Annu. Rev. Genet.*, **37**, 31–66.
2. Enzyme,A.N., Starts,W., Chains,D.N.A. and From,C. (1978) Primase, the dnaG protein of Escherichia coli. *J. Biol. Chem.*, **253**, 758–764.
3. Aravind,L., Leipe,D.D. and Koonin,E.V. (1998) Toprim — a conserved catalytic domain in type IA and II topoisomerases, DnaG-type primases, OLD Family nucleases and RecR proteins. *Nucleic Acids Res.*, **26**, 4205–4213.
4. Iyer,L.M., Koonin,E.V., Leipe,D.D. and Aravind,L. (2005) Origin and evolution of the archaeo-eukaryotic primase superfamily and related palm-domain proteins: structural insights and new members. *Nucleic Acids Res.*, **33**, 3875–3896.
5. García-Gómez,S., Reyes,A., Martínez-Jiménez,M.I., Chocrón,E.S., Mourón,S., Terrados,G., Powell,C., Salido,E., Méndez,J., Holt,I.J. *et al.* (2013) PrimPol, an archaic primase/polymerase operating in human cells. *Mol. Cell*, **52**, 541–553.
6. Rudd,S.G., Glover,L., Jozwiakowski,S.K., Horn,D. and Doherty,A.J. (2013) PPL2 translesion polymerase is essential for the completion of chromosomal DNA replication in the african trypanosome. *Mol. Cell*, **52**, 554–565.
7. Lipps,G., Röther,S., Hart,C. and Krauss,G. (2003) A novel type of replicative enzyme harbouring ATpase, primase and DNA polymerase activity. *EMBO J.*, **22**, 2516–2525.
8. Bocquier,A.A., Liu,L., Cann,I.K.O., Komori,K., Kohda,D. and Ishino,Y. (2001) Archaeal primase: bridging the gap between RNA and DNA polymerases. *Curr. Biol.*, **11**, 452–456.
9. Liu,L., Komori,K., Ishino,S., Bocquier,A.A., Cann,I.K.O., Kohda,D., Ishino,Y., Matsui,E., Nishio,M., Yokoyama,H. *et al.* (2003) Distinct domain functions regulating de Novo DNA synthesis of thermostable DNA primase from hyperthermophile pyrococcus horikoshii. *J. Biol. Chem.*, **42**, 14968–14976.
10. Lao-Sirieix,S.H. and Bell,S.D. (2004) The heterodimeric primase of the hyperthermophilic archaeon Sulfolobus solfataricus possesses DNA and RNA primase, polymerase and 3′-terminal Nucleotidyl transferase activities. *J. Mol. Biol.*, **344**, 1251–1263.
11. Galal,W.C., Pan,M., Kelman,Z. and Hurwitz,J. (2012) Characterization of DNA primase complex isolated from the archaeon, Thermococcus kodakaraensis. *J. Biol. Chem.*, **287**, 16209–16219.
12. Jozwiakowski,S.K., Borazjani Gholami,F. and Doherty,A.J. (2015) Archaeal replicative primases can perform translesion DNA synthesis. *Proc. Natl. Acad. Sci. USA*, **112**, E633–E638.
13. Crute,J.J., Tsurumi,T., Zhu,L.A., Weller,S.K., Olivo,P.D., Challberg,M.D., Mocarski,E.S. and Lehman,I.R. (1989) Herpes simplex virus 1 helicase-primase: a complex of three herpes-encoded gene products. *Proc. Natl. Acad. Sci. U.S.A.*, **86**, 2186–2189.
14. De Silva,F.S., Lewis,W., Berglund,P., Koonin,E.V. and Moss,B. (2007) Poxvirus DNA primase. *Proc. Natl. Acad. Sci. U.S.A.*, **104**, 18724–18729.
15. De Silva,F.S., Paran,N. and Moss,B. (2009) Products and substrate/template usage of vaccinia virus DNA primase. *Virology*, **383**, 136–141.
16. Mikhailov,V.S. and Rohrmann,G.F. (2002) Baculovirus replication factor LEF-1 is a DNA primase. *J. Virol.*, **76**, 2287–2297.
17. Bianchi,J., Rudd,S.G., Jozwiakowski,S.K., Bailey,L.J., Soura,V., Taylor,E., Stevanovic,I., Green,A.J., Stracker,T.H., Lindsay,H.D. *et al.* (2013) Primpol bypasses UV photoproducts during eukaryotic chromosomal DNA replication. *Mol. Cell*, **52**, 566–573.
18. Wan,L., Lou,J., Xia,Y., Su,B., Liu,T., Cui,J., Sun,Y., Lou,H. and Huang,J. (2013) hPrimpol1/CCDC111 is a human DNA primase-polymerase required for the maintenance of genome integrity. *EMBO Rep.*, **14**, 1104–1112.
19. Keen,B.A., Jozwiakowski,S.K., Bailey,L.J., Bianchi,J. and Doherty,A.J. (2014) Molecular dissection of the domain architecture and catalytic activities of human PrimPol. *Nucleic Acids Res.*, **42**, 5830–5845.
20. Prato,S., Vitale,R.M., Contursi,P., Lipps,G., Saviano,M., Rossi,M. and Bartolucci,S. (2008) Molecular modeling and functional characterization of the monomeric primase-polymerase domain from the Sulfolobus solfataricus plasmid pIT3. *FEBS J.*, **275**, 4389–4402.
21. Gill,S., Krupovic,M., Desnoues,N., Béguin,P., Sezonov,G. and Forterre,P. (2014) A highly divergent archaeo-eukaryotic primase from the Thermococcus nautilus plasmid, pTN2. *Nucleic Acids Res.*, **42**, 3707–3719.
22. Halgasova,N., Mesarosova,I. and Bukovska,G. (2012) Identification of a bifunctional primase-polymerase domain of corynephage BFK20 replication protein gp43. *Virus Res.*, **163**, 454–460.
23. Raoult,D., Audic,S., Robert,C., Abergel,C., Renesto,P., Ogata,H., La Scola,B., Suzan,M. and Claverie,J.M. (2004) The 1.2-megabase genome sequence of Mimivirus. *Science*, **306**, 1344–1350.
24. Legendre,M., Santini,S., Rico,A., Abergel,C. and Claverie,J.M. (2011) Breaking the 1000-gene barrier for Mimivirus using ultra-deep genome and transcriptome sequencing. *Virol. J.*, **8**, 1–6.
25. Kumar,S., Stecher,G. and Tamura,K. (2016) MEGA7: Molecular evolutionary genetics analysis version 7.0 for bigger datasets. *Mol. Biol. Evol.*, **33**, 1870–1874.
26. Biswas,T., Resto-Roldá,E., Sawyer,S.K., Artsimovitch,I. and Tsodikov,O.V. (2013) A novel non-radioactive primase-pyrophosphatase activity assay and its application to the discovery of inhibitors of Mycobacterium tuberculosis primase DnaG. *Nucleic Acids Res.*, **41**, 1–13.
27. Baykov,A.A. (1988) A malachite green procedure for orthophosphate determination and its use in alkaline Phosphatase-Based enzyme immunoassay. *Anal. Biochem.*, **270**, 266–270.
28. Ahn,S.J., Costa,J. and Emanuel,J.R. (1996) PicoGreen quantitation of DNA: Effective evaluation of samples pre- or post-PCR. *Nucleic Acids Res.*, **24**, 2623–2625.
29. Dragan,A.I., Casas-Finet,J.R., Bishop,E.S., Strouse,R.J., Schenerman,M.A. and Geddes,C.D. (2010) Characterization of PicoGreen interaction with dsDNA and the origin of its fluorescence enhancement upon binding. *Biophys. J.*, **99**, 3010–3019.
30. Koepsell,S.A., Hanson,S., Hinrichs,S.H. and Griep,M.A. (2005) Fluorometric assay for bacterial primases. *Anal. Biochem.*, **339**, 353–355.
31. Ghodke,P.P., Bommisetti,P., Nair,D.T. and Pradeepkumar,P.I. (2019) Synthesis of N2-Deoxyguanosine Modified DNAs and the Studies on Their Translesion Synthesis by the E. coli DNA Polymerase IV. *J. Org. Chem.*, **84**, 1734–1747.
32. Liu,L., Komori,K., Ishino,S., Bocquier,A.A., Cann,I.K.O., Kohda,D. and Ishino,Y. (2001) The archaeal DNA primase: Biochemical characterization of the p41-p46 complex from pyrococcus furiosus. *J. Biol. Chem.*, **276**, 45484–45490.
33. Lucchini,G., Francesconi,S., Foiani,M., Badaracco,G. and Plevani,P. (1987) Yeast DNA polymerase–DNA primase complex; cloning of PRI 1, a single essential gene related to DNA primase activity. *EMBO J.*, **6**, 737–742.
34. Lao-Sirieix,S.H., Nookala,R.K., Roversi,P., Bell,S.D. and Pellegrini,L. (2005) Structure of the heterodimeric core primase. *Nat. Struct. Mol. Biol.*, **12**, 1137–1144.

35. Steitz,T.A. (1999) DNA polymerases: structural diversity and common mechanisms. *J. Biol. Chem.*, **274**, 17395–17398.

36. Martínez-Jiménez,M.I., García-Gómez,S., Bebenek,K., Sastre-Moreno,G., Calvo,P.A., Díaz-Talavera,A., Kunkel,T.A. and Blanco,L. (2015) Alternative solutions and new scenarios for translesion DNA synthesis by human PrimPol. *DNA Repair (Amst).*, **29**, 127–138.

37. Jones,S.A. and Hu,J. (2013) Protein-Primed terminal transferase activity of hepatitis B virus polymerase. *J. Virol.*, **87**, 2563–2576.

38. Le Breton,M., Henneke,G., Norais,C., Flament,D., Myllykallio,H., Querellou,J. and Raffin,J.P. (2007) The heterodimeric primase from the euryarchaeon pyrococcus abyssi: a multifunctional enzyme for initiation and repair? *J. Mol. Biol.*, **374**, 1172–1185.

39. Beckman,R.A., Mildvan,A.S. and Loeb,L.A. (1985) On the fidelity of DNA replication: manganese mutagenesis in vitro†. *Biochemistry*, **24**, 5810–5817.

40. Frank,E.G. and Woodgate,R. (2007) Increased catalytic activity and altered fidelity of human DNA polymerase ι in the presence of manganese. *J. Biol. Chem.*, **282**, 24689–24696.

41. Motea,E.A. and Berdis,A.J. (2010) Terminal deoxynucleotidyl transferase: The story of a misguided DNA polymerase. *Biochim. Biophys. Acta - Proteins Proteom.*, **1804**, 1151–1166.

42. Fowler,J.D. and Suo,Z. (2006) Biochemical, structural, and physiological characterization of terminal deoxynucleotidyl transferase. *Chem. Rev.*, **106**, 2092–2110.

43. Della,M., Palmbos,P.L., Tseng,H.M., Tonkin,L.M., Daley,J.M., Topper,L.M., Pitcher,R.S., Tomkinson,A.E., Wilson,T.E. and Doherty,A.J. (2004) Mycobacterial Ku and ligase proteins constitute a two-component NHEJ repair machine. *Science*, **306**, 683–685.

44. Gong,C., Bongiorno,P., Martins,A., Stephanou,N.C., Zhu,H., Shuman,S. and Glickman,M.S. (2005) Mechanism of nonhomologous end-joining in mycobacteria: A low-fidelity repair system driven by Ku, ligase D and ligase C. *Nat. Struct. Mol. Biol.*, **12**, 304–312.

45. Ranjith-Kumar,C.T., Gajewski,J., Gutshall,L., Maley,D., Sarisky,R.T. and Kao,C.C. (2001) Terminal nucleotidyl transferase activity of recombinant flaviviridae RNA-Dependent RNA polymerases: Implication for viral RNA synthesis. *J. Virol.*, **75**, 8615–8623.

46. Zafar,M.K., Ketkar,A., Lodeiro,M.F., Cameron,C.E. and Eoff,R.L. (2014) Kinetic analysis of human PrimPol DNA polymerase activity reveals a generally error-prone enzyme capable of accurately bypassing 7,8-dihydro-8-oxo-2′-deoxyguanosine. *Biochemistry*, **53**, 6584–6594.

47. Vaisman,A. and Woodgate,R. (2015) 1. Ribonucleotide selectivity of translesion synthesis DNA polymerases. *Crit. Rev. Biochem. Mol. Biol.*, **661**, 1–23.

48. Su,Y., Egli,M. and Guengerich,F.P. (2016) Mechanism of ribonucleotide incorporation by human DNA polymerase η. *J. Biol. Chem.*, **291**, 3747–3756.

49. Crespan,E., Furrer,A., Rösinger,M., Bertoletti,F., Mentegari,E., Chiapparini,G., Imhof,R., Ziegler,N., Sturla,S.J., Hübscher,U. *et al.* (2016) Impact of ribonucleotide incorporation by DNA polymerases β and δ on oxidative base excision repair. *Nat. Commun.*, **7**, 10805.

50. Cilli,P., Minoprio,A., Bossa,C., Bignami,M. and Mazzei,F. (2015) Formation and repair of mismatches containing ribonucleotides and oxidized bases at repeated DNA sequences. *J. Biol. Chem.*, **290**, 26259–26269.

51. Mentegari,E., Crespan,E., Bavagnoli,L., Kissova,M., Bertoletti,F., Sabbioneda,S., Imhof,R., Sturla,S.J., Nilforoushan,A., Hübscher,U. *et al.* (2017) Ribonucleotide incorporation by human DNA polymerase ν impacts translesion synthesis and RNase H2 activity. *Nucleic Acids Res.*, **45**, 2600–2614.

52. Nick McElhinny,S.A. and Ramsden,D.A. (2003) Polymerase Mu Is a DNA-Directed DNA/RNA Polymerase. *Mol. Cell Biol.*, **23**, 2309–2315.

53. Traut,T.W. (1994) Physiological concentrations of purines and pyrimidines. *Mol. Cell Biochem.*, **140**, 1–22.

54. Suzan-Monti,M., La Scola,B., Barrassi,L., Espinosa,L. and Raoult,D. (2007) Ultrastructural characterization of the giant volcano-like virus factory of Acanthamoeba polyphaga Mimivirus. *PLoS One*, **2**, e328.

55. Renesto,P., Abergel,C., Decloquement,P., Moinier,D., Azza,S., Ogata,H., Fourquet,P., Gorvel,J.-P. and Claverie,J.-M. (2006) Mimivirus giant particles incorporate a large fraction of anonymous and unique gene products. *J. Virol.*, **80**, 11678–11685.

56. Legendre,M., Poirot,O., Hingamp,P., Seltzer,V., Byrne,D., Lartigue,A., Lescot,M., Bernadac,A., Poulain,J., Abergel,C. *et al.* (2010) mRNA deep sequencing reveals 75 new genes and a complex transcriptional landscape in Mimivirus. *Genome Res.*, **20**, 664–674.

57. Mutsafi,Y., Zauberman,N., Sabanay,I. and Minsky,A. (2010) Vaccinia-like cytoplasmic replication of the giant Mimivirus. *Proc. Natl. Acad. Sci. U.S.A.*, **107**, 5978–5982.

58. Sale,J.E., Lehmann,A.R. and Woodgate,R. (2012) Y-family DNA polymerases and their role in tolerance of cellular DNA damage. *Nat. Rev. Mol. Cell Biol.*, **13**, 141–152.

59. Guilliam,T.A., Jozwiakowski,S.K., Ehlinger,A., Barnes,R.P., Rudd,S.G., Bailey,L.J., Skehel,J.M., Eckert,K.A., Chazin,W.J. and Doherty,A.J. (2015) Human PrimPol is a highly error-prone polymerase regulated by single-stranded DNA binding proteins. *Nucleic Acids Res.*, **43**, 1056–1068.

60. Guilliam,T.A., Bailey,L.J., Brissett,N.C. and Doherty,A.J. (2016) PolDIP2 interacts with human PrimPol and enhances its DNA polymerase activities. *Nucleic Acids Res.*, **44**, 3317–3329.